3rd International Conference on Tomography of Materials and Structures
Lund, Sweden, 26-30 June 2017, ICTMS2017-76

Microstructure and Failure Analysis During Granular Compaction Using X-ray CT and 3D X-ray Diffraction

Ryan C. Hurley *[1], Jonathan Lind[1], Minta C. Akin[1], Darren Pagan[1], Eric B. Herbold[1], Michael A. Homel[1], and Ryan Crum[1]

[1]Lawrence Livermore National Laboratory, Livermore, CA 94550, USA

Keywords: x-ray tomography, three-dimensional x-ray diffraction, granular materials, microstructure

Summary: We combine X-ray computed tomography and 3D X-ray diffraction to measure grain-resolved strains, kinematics, and contact fabric in two granular samples undergoing quasi-static compaction. Our measurements enable construction of porosity fields, contact and force networks, and grain states preceding fracture. We provide statistics and a discussion of these microstructural variables.

1. INTRODUCTION

Stiff, frictional granular materials have been extensively studied numerically, but an understanding of their structure-property relations, their interparticle load-bearing contact network, and their mechanics during compaction, remains elusive and has yet to be thoroughly examined experimentally. Recent advances in X-ray computed tomography (XRCT) and 3D X-ray diffraction (3DXRD) [1] permit high-resolution co-located measurements of grain strain, kinematics, and contact fabric in granular and polycrystalline materials. These measurements facilitate in situ studies of microstructure evolution in granular materials by enabling calculation of local porosity, strain, contact and force networks [2]. Here, we combine XRCT and 3DXRD to study micromechanics and failure during compaction of two granular samples. We provide statistics of the local porosity and stress states of individual grains and discuss the reconstruction of force networks and their utility in investigating structure-property relations and constitutive laws.

2. EXPERIMENTAL METHOD

Two granular samples were prepared by pouring particles into 1.5mm inner diameter Al-6061 tubes and placing them in the compact load frame present at beamline 1-ID-E of the Advanced Photon Source (APS) [3]. The first sample contained 989 bidisperse single-crystal sapphire grains with diameters 200 μm and 165 μm. The second sample contained single-crystal sapphire grains mixed with copper. Each sample was subjected to displacement-controlled quasi-static uniaxial compaction to failure. At intervals of approximately 20-30 N, displacement was held constant while 1 mm tall sections of each sample were illuminated by a 52 keV monochromatic X-ray beam. For each 1 mm tall section, samples were rotated twice through 360°, pausing at 0.2° increments while a Retiga 4000 CCD camera captured transmission radiographs during the first rotation a GE-41RT area detector captured diffraction spots during the second rotation. An Inverse Radon Transform was employed to construct XRCT images of each sample at each load step. A diffraction peak search algorithm was combined with a minimization procedure (similar to [1]) to extract grain positions, lattice orientations, and elastic strains.

Raw XRCT images had a resolution of 0.74 μm per voxel. Sapphire grains were segmented from XRCT images using circular Hough transforms on each layer of the image. Aligned circles from adjacent slices with similar radii and positions were merged and voxels falling within these shells were assigned a unique label. Grain positions and volumes were found by averaging voxel positions and summing voxel counts for each label, respectively. Contact points between grains were identified as voxels whose local 27 voxel neighborhood contained different grain labels. Normal and tangent basis vectors for each contact plane were determined by using these contact points and grain centroids. Grain stress tensors, σ_i, were assigned to each segmented grain by aligning XRCT and 3DXRD coordinate frames and computing $\sigma_i = C_{ij}\epsilon_j$, where C_{ij} is the stiffness tensor

*e-mail: hurley10@llnl.gov

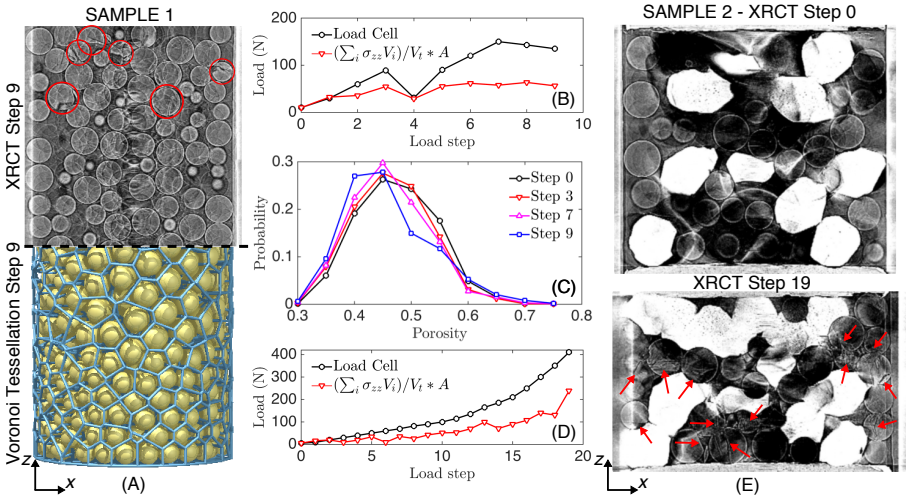

Figure 1: (A) XRCT and rendered segmentation, with Voronoi tessellation, of sample 1 at load step 9. (B) Load cell and sample stress data from 3DXRD. V_i is grain volume, V_t is total sample volume, A is piston area. (C) Local porosity as a function of load for sample 1. (D) Same as (B) but for sample 2. (E) XRCT for sample 2, load steps 0 and 19, showing the large deformation of copper and widespread fracture of sapphire grains.

for sapphire and ϵ_j is the grain strain from 3DXRD. Grain stresses and contact planes were employed in an optimization problem [2] to calculate inter-particle forces at each grain-grain and grain-boundary contact.

3. RESULTS

Figure 1A shows sample 1 at load step 9. The upper half shows a $x-z$ plane cut through the center of the XRCT image. Fractured grains are highlighted in red and occur near the top piston. The stress, local porosity, and contact force states of these grains were tracked before and, when possible, after fracture using 3DXRD and XRCT data. The bottom half of Fig. 1A shows a segmented rendering of the sample and edges of a radical Voronoi tessellation computed using Voro++ [4]. This tessellation was used to determine local grain porosity, ϕ_i, by $\phi_i = 1 - V_i/V_c$, where V_i is the grain volume and V_c is the Voronoi cell volume. Figure 1C shows the evolution of the probability distribution of porosity as a function of load step, revealing a porosity reduction at higher loads. Figure 1B shows the load cell data and volume-averaged grain stress as a function of load step. Both data sets demonstrate similar trends; lower volume-averaged stresses indicate non-uniform values of vertical grain stress, σ_{zz}, and possible load transmission through the Al-6061 tube.

Figure 1D shows the load cell data and volume-averaged grain stress (averaged only over sapphire grains) of sample 2 as a function of load step. As for sample 1, lower volume-averaged stresses indicate non-uniform stress and load transmission through the Al-6061 tube. The lower value may also reflect the absence of copper stress for this sample: copper strains were unavailable because copper plasticity at low loads led to Deybe-Scherrer rings rather than diffraction peaks. Figure 1E shows XRCT images for load steps 0 and 19. Copper grains, shown as large white features, can be observed undergoing large deformation and coalescence, while sapphire grains exhibit widespread fracture and comminution as highlighted by red arrows.

The authors acknowledge Lawrence Livermore National Laboratory's LDRD program grants numbered 16-ERD-010 and 17-LW-009. This work was performed under the auspices of the U.S. Department of Energy by Lawrence Livermore National Laboratory under Contract DE-AC52-07NA27344. LLNL-ABS-719811.

References

[1] J. Oddershede, S. Schmidt, H.F. Poulsen, H.O. Sorensen, J. Wright, & W. Reimers. Determining grain resolved stresses in polycrystalline materials using three-dimensional X-ray diffraction. *Journal of Applied Crystallography* 43(3), 539-549, 2010.

[2] R.C. Hurley, S.A. Hall, J.E. Andrade, & J. Wright. Quantifying Interparticle Forces and Heterogeneity in 3D Granular Materials. *Physical Review Letters* 117(9), 098005, 2016.

[3] https://www1.aps.anl.gov/sector-1/1-id

[4] C. Rycroft. A three-dimensional Voronoi cell library in C++. *Lawrence Berkeley National Laboratory*, 2009.